

On the electronic structure and magnetism of CaCrO_3 : a hybrid-exchange density-functional-theory study

Jiawei Chang^{1,2}, Qiuyuan Chen^{1,2}, Lin Ma^{1,2}, Chenghan Li^{1,2}, Yicheng Peng¹, Wei Wu^{3*}, and Hai Wang^{1*}

¹Key Laboratory of Yunnan Provincial Higher Education Institutions for Organic Optoelectronic Materials and Devices, Kunming University, People's Republic of China

²School of Physics and Technology, Kunming University, Kunming 650091, People's Republic of China

³UCL Department of Physics and Astronomy and London Centre for Nanotechnology, University College London, Gower Street, London WC1E 6BT, United Kingdom

wei.wu@ucl.ac.uk

wanghai_lab@sina.com

ABSTRACT

Recently the perovskite oxide CaCrO_3 has raised concerns for its ground-state electronic structure and magnetic properties. In this report, the hybrid-exchange density functional, PBE0, is used to calculate the electronic structure and magnetic properties of CaCrO_3 . The ferromagnetic, A-type anti-ferromagnetic, C-type anti-ferromagnetic, and G-type anti-ferromagnetic states (defined in the text) have been investigated carefully. The computed magnetic ground state has a G-type anti-ferromagnetic configuration (the Néel state). The calculation result is that the nearest-neighbor exchange interactions in the ab -plane and along the c -axis are antiferromagnetic. The next-nearest-neighbor exchange interaction in the ab -plane is much weak but ferromagnetic. We hope this work would shed some light on the controversial ground state of CaCrO_3 .

KEY WORDS: CaCrO₃, magnetism, electronic structure, hybrid-exchange density functional

I. INTRODUCTION

Transition-metal oxides (TMOs) are an important family of strongly correlated materials in condensed matter physics [S. Cheong and M. Mostovoy, Nat. Mat. 6, 13 (2007)]. For example, yttrium-barium-copper-oxide (YBCO) is the first high-transition-temperature (unconventional) superconductor (HTSC) ever found [1]. This surprising yet challenging discovery [1] has triggered extensive experimental and theoretical efforts on YBCO and other related TMOs both for fundamental physics research and practical applications of HTSC. Moreover, chromium dioxide (CrO₂), is half metallic (one spin channel is conducting, while the other insulating), which has great potential for storing and transporting information encoded in the electron spin in spintronics [2]. In addition, TMOs have many other applications such as multiferroics [S. Cheong and M. Mostovoy, Nat. Mat. 6, 13 (2007)], transparent conductors [S. C. Dixon, D. O. Scanlon, C. J. Carmalt, and I. P. Parkin, J. Mater. Chem. C, 4, 6946 (2016)], advanced ceramics [N. P. Padture, Nat. Mat. 15, 804 (2016)] and high-dielectric-constant (high- κ) materials [J. Robertson, Rep. Prog. Phys. 69, 327 (2006)]. The attractive physical properties and promising potentials in material technology of TMOs are closely related to (i) the short-range exchange interaction between *d*-electrons of transition-metal ions, which

is mediated by the p -electrons of oxygen, (ii) the orbital degrees of freedom, essentially the ordering of orbitals, and (iii) spin-orbit interaction that could be important for determining the magnetic ground state. Orbital ordering can be defined as either (i) orbitals with one orientation and the other orientation are alternately and regularly arranged or (ii) different orbitals are arranged regularly.

The Cr^{4+} -based perovskites including CaCrO_3 , PbCrO_3 and SrCrO_3 have recently attracted considerable attention [3-9]. Especially in CaCrO_3 (the crystal structure is given in Fig. 1), the complex interaction between magnetism and conductivity as well as lattice vibration in CaCrO_3 plays an important role to have a unambiguous view of the electronic ground state [3, 4]. The issue of whether CaCrO_3 is metallic or insulating remains a matter of dispute, which is related to the magnetic Cr^{4+} -based perovskites structure in the ground state. Comprehensive experimental studies have shown that the unstable Cr-O bond in CaCrO_3 leads to abnormal properties, which may cause the change of electronic properties from localized behavior to delocalized [3]. In Ref.[3], CaCrO_3 was characterized by magnetic and resistance experiments as insulators but subject to chemical-bond instability that will affect the ground-state properties.

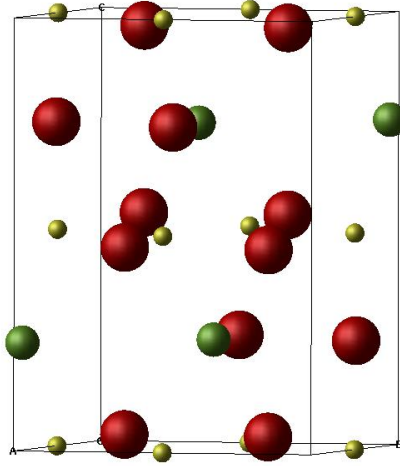


FIG. 1: (Color on line.) The conventional cell of perovskite CaCrO_3 is shown. Ca is depicted as a green ball, O as red, and Cr as yellow.

Another study, combining experiments and first-principles calculations, has shown that CaCrO_3 is a rare case of anti-ferromagnetic (AFM) metal owing to the co-existence of anti-ferromagnetism and metallic-like conductivity [4, 5]. However, the experimental evidence for the claim of is vague; the authors have provided indirect observation through extrapolation of the optical reflectance data. The theoretical work supporting the C-type AFM state, in which the spin is ferromagnetic (FM) order along the c -axis, while the AFM is the ground state in the ab -plane, in the framework of LSDA (local spin density approximation) + U suggest that the electronic structure of CaCrO_3 is strongly dependent on the way to treat the electron correlations [6]. The electronic state was predicted to be metallic within LSDA, but insulating once an appropriate value of U was included. Another set of first principles based on GGA (generalized gradient approximation) + U [7] have shown that the C-type

AFM is metallic in the intermediate U . However this depends on the orientation of spins [7]; the so-called the C_y -AFM state with the spin pointing to [001] direction is the ground state with $U=1.4$ eV. This suggests the magnetic ground state is fragile and complicated for CaCrO_3 . A recent experimental work has shown that it is possible there could exist Bose-Einstein condensate associated with orbital degrees of freedom in CaCrO_3 [8]. To the best knowledge of the authors, most of the previous theoretical work was carried out in the framework of the pure density functional theory (DFT) or DFT+ U . The electronic correlation can be taken into account by including U parameter in DFT, as performed previously [6, 7]. On the other hand, hybrid-exchange functional, such as PBE0 [9], would also be able to include electronic correlations by mixing exact Fock exchange with that from GGA exchanges functionally. This can not only provide an alternative route to compute the ground-state properties, but also theoretical insight from a different perspective. Recently, DFT calculations based on HSE functional and DFT + U methods for CaCrO_3 and other perovskite oxides have been compared [10]. However, therein the research focus is on the electrocatalysis and doped materials rather pristine ones [10].

In this paper, the electronic structure of CrO_2 is first benchmarked within the theoretical framework of PBE0 [9], which is a hybrid exchange density functional without any adjustable parameters. Following this, the

electronic structure and magnetic properties of CaCrO_3 were then calculated systematically.

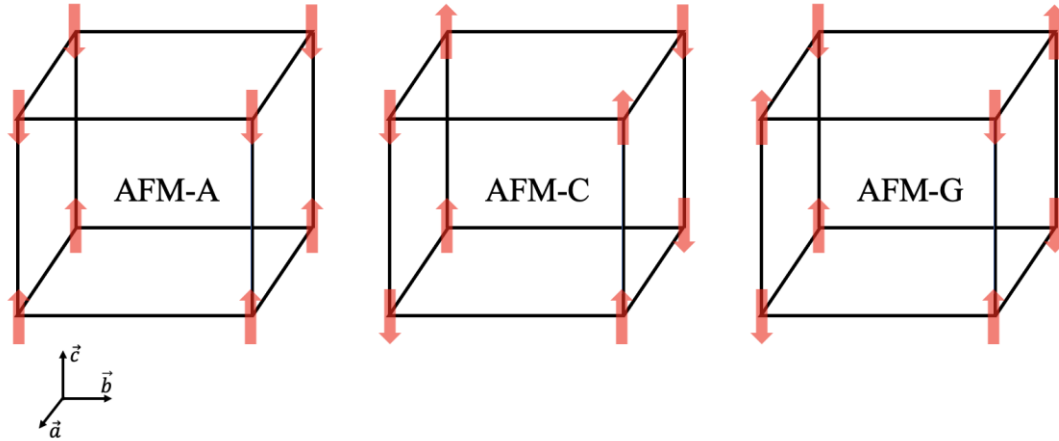


FIG.2: The spin configurations AFM-G, AFM-C, and AFM-G as defined in the text. AFM-A refers to the spin configurations in which FM in the ab plane and AFM along the c -axis, AFM-C AFM in the ab plane and FM along the c -axis, and AFM-G is the Néel state, both AFM in the ab plane and the c -axis.

The total energies of FM, the A-type AFM states (AFM-A, AFM along the c -axis yet FM on the ab -plane), the C-type (AFM-C) and the G-type AFM (Néel state, AFM-G state) are calculated carefully. The spin configurations for these three types of AFM states are illustrated in Fig.2. By comparing the total energies of these magnetic states, the nearest neighboring (NN) and next nearest neighboring (NNN) exchange interactions can be extracted. In this paper we have found that the AFM-G state is the magnetic ground state without taking into account the spin-orbit interaction, which is different that viewed as well as foretold in Ref. [4]. However, the total energy difference is ~ 30 meV, which is comparable to the energy scale of the room temperature, which suggests the importance of lattice vibrations and thermal fluctuations for the determination of the

ground-state properties. The calculations of exchange interactions suggest that there are anti-ferromagnetic interaction both in the ab -plane and along the c -axis. The rest of the discussion is arranged as follows: the computational details are given in the section II, the calculation results are shown and discussed in the section III, and some more general conclusions are drawn in the section IV.

II. COMPUTATIONAL DETAILS

The electronic structures and magnetic properties of CrO_2 and CaCrO_3 were calculated by the DFT and the hybrid-exchange functional PBE0 implemented in crystal 09 code [11]. Here we use the experimental lattice parameters and symmetry ($Pbnm$) and atomic coordinates reported in Ref. [12]. The basis sets of Ca [13], Cr [14] as well as O [15], used for solid-phase computations, are employed here. For the Monkhorst-Pack sampling of the first Brillouin zone [16], we have chosen the coefficient set $7 \times 7 \times 5$, which is consistent with the ratio of spatial lattice parameters. The operation of Coulomb and exchange Series in direct space can be controlled by setting the Gaussian overlap tolerance to 10^{-6} , 10^{-6} , 10^{-6} , 10^{-6} and 10^{-12} [11]. The self-consistent field (SCF) process converges to a 10^{-7} a. u. tolerance of the total energy. In order to accelerate the convergence of the SCF process, 30% linear mixture of Fock matrix is used in all the calculations here. PBE0 mixed exchange function is used to describe electronic exchange and correlation [9].

Electron exchanges and correlation are described by PBE0 hybrid-exchange functional [9]. In addition to partially eliminating the self-interaction error, PBE0 functional also balances the delocalization and localization of wave functions by mixing a quarter of the exact Fock exchange with the generalized gradient approximation (GGA) exchange related functional [9]. This type of hybridization, such as B3LYP or PBE0, has been shown to accurately describe the electronic structure and magnetic properties of inorganic and organic compounds [18,19].

The Heisenberg model [17] for the spin-spin interactions in CaCrO_3 is defined here as,

$$\hat{H} = J_c \sum_{ij \in c} \hat{\vec{S}}_i \cdot \hat{\vec{S}}_j + J_{ab} \sum_{ij \in (ab)} \hat{\vec{S}}_i \cdot \hat{\vec{S}}_j + J'_{ab} \sum_{ij \in (ab)'} \hat{\vec{S}}_i \cdot \hat{\vec{S}}_j, \quad (1)$$

Here J_c represents the NN exchange interaction along the c -axis, J'_{ab} (J_{ab}) between the NN (NNN) in the ab -plane. Here, i and j marks the positions of Cr ions. These exchange interactions can be computed as below,

$$\begin{aligned} E_{FM} - E_a &= 8S^2 J_c, \\ E_{FM} - E_c &= 16S^2 (J_{ab} + J'_{ab}), \\ E_{FM} - E_g &= 8S^2 J_c + 16S^2 J_{ab}, \end{aligned} \quad (2)$$

Among them, E_{FM} , E_a , E_c and E_g are the entire energies of FM, AFM-A, AFM-C and AFM-G states, respectively. Here Cr^{4+} ions are assumed to

carry spin-1 ($S = 1$).

III. RESULTS AND DISCUSSIONS

A. Benchmark: the electronic structure of CrO_2

First, the electronic structure of CrO_2 has been benchmarked for the AFM and FM spin configurations. The zero-energy is set to be the Fermi energy. The DFT calculations based on PBE0 functional have predicted that (i) its ground state is FM, and (ii) it is a half metal as shown in Fig.3. This result is consistent with the previous experimental and theoretical results [2]. The projected density of states (PDOS) onto the d -orbitals suggests that the conduction band is dominated by the d -electrons. This can provide a strong evidence that PBE0 functional can be employed for such a transition-metal oxide system, providing reliable computational results.

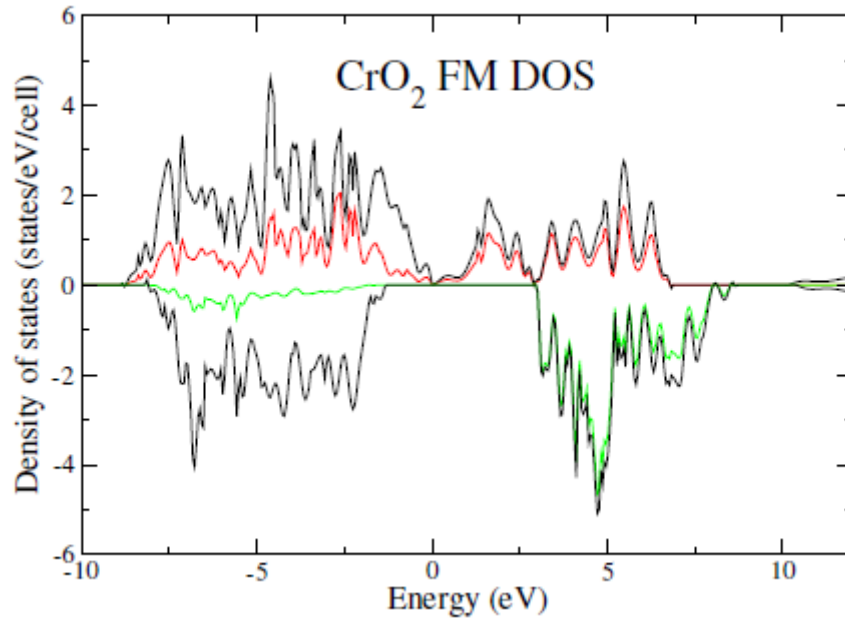


FIG. 3: (Colour on line.) FM DOS for CrO_2 is plotted from -10 to 12 eV with positive (negative) representing spin-up (spin-down). The total DOS is depicted in black. The

spin-up (spin-down) PDOS to Cr d -orbitals is depicted in red (green). As suggested by the DOS, CrO_2 is a half metal.

B. The electronic structure of CaCrO_3

The PDOS of the three states of AFM-A, AFM-C, and AFM-G on Cr (the first row) d -orbital, O (the second row) p -orbital and spin density (the third row) are shown in Fig. 4. The electronic states of FM, AFM-A, AFM-C and AFM-G were predicted to be insulating, as shown in Fig.4. The computed band gap in AFM-C (Fig.3b) is ~ 2.3 eV which is slightly smaller than those in AFM-A and AFM-G (~ 2.5 eV, Fig.4a and c, respectively). For such size of band gap, the electrical conductivity can be easily dominated by the defects that can be readily thermally excited. The energy of the valence band maximum (VBM) is set to 0. The total energies per unit cell of AFM-A, AFM-C, and AFM-G states are lower than that of FM by 36.87, 32.93, and 74.08 meV, respectively. The AFM-G is the most stable state, but the energy differences between the three kinds of AFM states are up ~ 38 meV, draw near the energy scale of the indoor temperature, indicating the significance of thermal fluctuations. Compared with the previous work, these results are in parity from the academic calculations and experiment research [4]. In particular, the difference in the energy between AFM-A and AFM-C is only about ~ 4 meV. Thus, given the influence of lattice vibration and thermal fluctuation, the stability of the magnetic state is fragile. This will further lead to disordered magnetic properties, thus preventing proper observation of CaCrO_3 electronic states.

The computed spin densities on Cr are approximately $2 \mu_B$. The PDOS near the VBM suggests that the d -orbitals including $d_{x^2-y^2}$, d_{xz} , d_{yz} are dominant. By comparing the PDOS of the d -orbital and p -orbital, it can be found that there may be a strong hybridization between them, especially near VBM.

From the spin density of AFM-A (Fig.4g), it can be seen that the spins are anti-aligned along the c -axis, but aligned on the ab -plane. In AFM-C (Fig.4h), the spins are aligned along the c -axis, but in the opposite direction in the ab -plane. In AFM-G, the spins in the ab -plane and along the c -axis are both anti-aligned. Although there are significant differences between the spin states, they all have a common feature, i.e. anti-ferro-orbital ordering (AFOO, indicated by yellow arrow) is present in the ab -plane, and the OO along the c -axis is not obvious.

	AFM-A	AFM-C	AFM-G
d_{z^2}	0.11	0.11	0.11
d_{xz}	0.52	0.55	0.51
d_{yz}	0.54	0.53	0.56
$d_{x^2-y^2}$	0.60	0.69	0.51
d_{xy}	0.13	0.14	0.14

TABLE 1: Projected spin density of AFM-A, atomic AFM-C and atomic AFM-G states on Cr d -orbitals.

The spin density projected onto the d -orbital is also considered. The spin density is mainly determined by the d_{xz} , d_{yz} , and $d_{x^2-y^2}$ orbitals (these

three orbitals are $\sim 1.7\mu_B$), as given in Table I. $d_{x^2-y^2}$ population is strengthened largely in AFM-C state as compared to AFM-G and AFM-A states. The d_{xz} , d_{yz} , and $d_{x^2-y^2}$ orbitals are all nearly half-filled, which suggests the magnetic properties are dominated by itinerant d -electrons. This is consistent with the discussions in Ref. [8].

C. Exchange interaction

By comparing the total energy of the above four magnetic states according to the eq.2, the exchange interactions defined in the eq.1 can be obtained. The computed J_c is 1.15 meV, J_{ab} 0.58 meV, and J_{ab}' -0.07 meV. Notice that the NNN exchange interaction in the ab -plane is much weaker than the NN one, which is reasonable. The spins are coupled with a NN antiferromagnetic couplings along the c -axis, and the NN exchange interaction in the ab -plane is AFM as well. However, the NNN exchange interaction is weak FM.

Comparison with the previous experiments

The computed PDOS is conform with the previous x-ray absorption spectroscopy (XAS), which had shown in Fig.2a of Ref. [5]. The predicted energy difference between the peak d -orbital and O p -orbitals is $\sim 3.7\text{eV}$, slightly less than the measured energy difference ($\sim 5\text{ eV}$). More advanced computational methods, something like GW [20], are required to improve the description of the theory. However, this is not the main topic of this

article. The Néel temperature T_N can be measured by $1/\chi$ versus T curve, and the measured value was approximately 90 K in Ref.[3, 4]. It can lead to a similar exchange interaction as the calculated result of exchange interactions J_c and J_{ab} (~ 0.97 meV) according the mean-field expression for the transition temperature $\theta = zJS(S + 1)/3k_B$ (here $z=4$ and $S=2$). In addition, the calculated magnetic moment of approximately $2.0\mu_B$ is much smaller than the observed magnetic moment ($3.7\mu_B$) [3]. This might be due to the out-plane spin anisotropy, which was not taken into account here. However, $1.2 \mu_B$ has been observed in Ref.[4], which indicates the possible existence of iterative magnetism. An alternative explanation for this reduced magnetic moment is the in-plane magnetic anisotropy (rather out-plane anisotropy), induced by the local crystal field. We can also see that the orbital ordering in the ab -plane, which seems uncorrelated with the overall spin ordering.

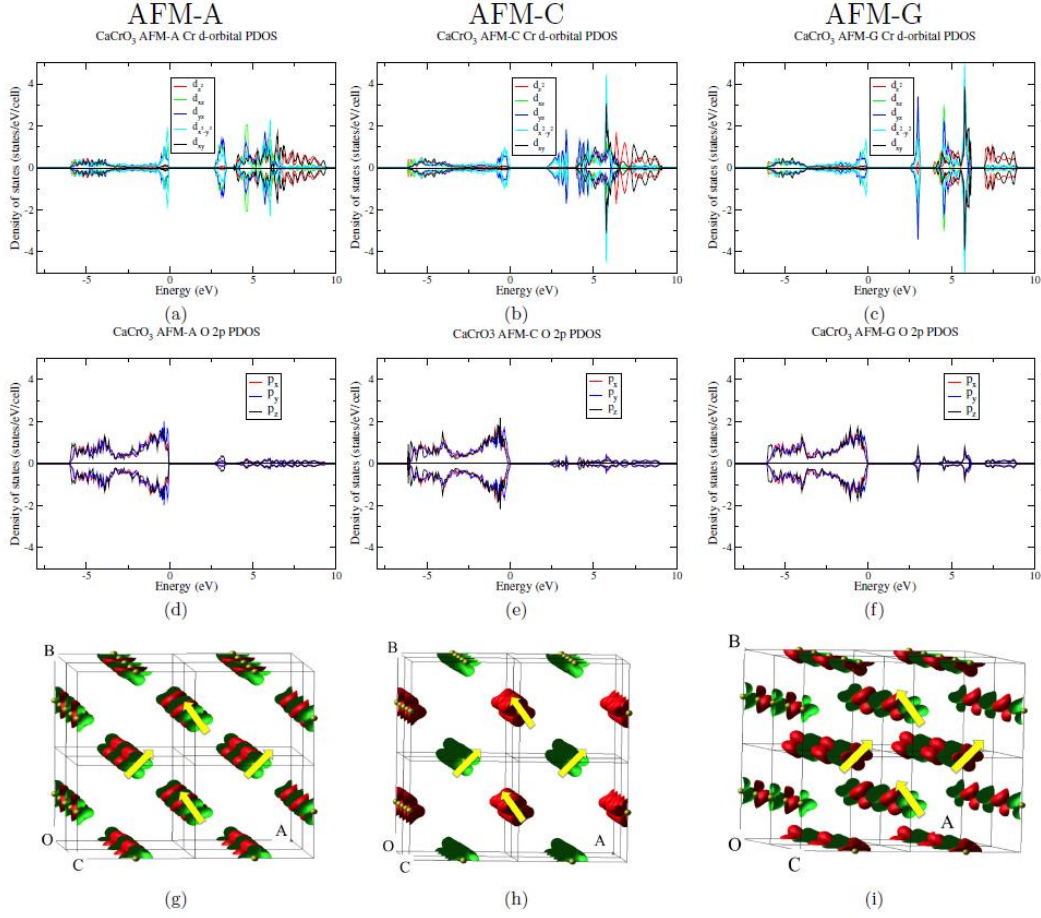


FIG. 3: The PDOS of the type-A, type-C and type-G AFM of CaCrO_3 with spin density on Cr d -orbital (a-c), O $2p$ orbital (d-f) and Cr atoms (g-i) are represented by lines of different colors, respectively. The PDOS of d_{z^2} , d_{xz} , d_{yz} , $d_{x^2-y^2}$ and d_{xy} are red, green, blue, cyan and black, respectively. The PDOS for $2p_x$, $2p_y$, and $2p_z$ are shown in red, blue, and black, respectively. The VBM is chosen to be zero energy. The spin-up spin densities are in red, the spin-down in blue. The direction of the orbital is shown by the yellow arrow, and notice that in the ab -plane the orbitals are anti-ferro-ordered.

IV. CONCLUSION

To sum up, the Cr^{4+} -based perovskite oxide CaCrO_3 has been modeled by using hybrid-exchange density functional PBE0 within the DFT for the electronic structure and magnetic properties. The results of the exchange interaction show that the spins are coupled with AFM exchange interactions both along the c -axis and in the ab -plane there. The PDOS has

already implied that between the $3d$ and $2p$ orbitals there exist a massive hybridization. However, the role of the NNN FM exchange interaction is not dominant. In the future, it may be worthwhile to use more advanced strongly-correlation methods such as dynamical mean-field theory [21] for this type of systems, and we hope it will stimulate more discussion with regard to this fascinating material.

V. ACKNOWLEDGEMENT

We gratefully acknowledge Prof. Gong Hao (National University of Singapore) for helpful discussions. We thank the funding from the National Natural Science Foundation of China (Nos. 11564023 ,51904137), Yunnan local University Joint Special Funds for Basic Research (2017FH001-007 and 2018FH001-017), the Applied Basic Research Projects of Yunnan Province (2019FD044), Scientific Research Fund of Yunnan Education Department (2019J0563, 2019J0564, 2020Y0464, 2021Y704, 2021Y711, and 2021Y713), and UK Research Councils Basic Technology Programme under grant EP/F041349/1. I thank Bo Chen for stimulating discussions.

DATA AVAILABILITY

The data that support the findings of this study are available from the corresponding author upon reasonable request.

REFERENCES:

- [1] M.K. Wu, J.R. Ashburn, C.J. Torng, P.H. Hor, R.L. Meng, L. Gao, Z.J. Huang, Y.Q. Wang, C.W. Chu, *Physical Review Letters*, 58 (1987) 908-910.
- [2] J.M.D. Coey, M. Venkatesan, *Cheminform*, 91 (2002) 8345-8350.
- [3] J.S. Zhou, C.Q. Jin, Y.W. Long, L.X. Yang, J.B. Goodenough, *Phys Rev Lett*, 96 (2006) 046408.
- [4] S.V. Streltsov, M.A. Korotin, V.I. Anisimov, D.I. Khomskii, *Physical Review B*, 78 (2008).
- [5] P.A. Bhobe, A. Chainani, M. Taguchi, R. Eguchi, M. Matsunami, T. Ohtsuki, K. Ishizaka, M. Okawa, M. Oura, Y. Senba, H. Ohashi, M. Isobe, Y. Ueda, S. Shin, *Physical Review B*, 83 (2011).
- [6] A.C. Komarek, S.V. Streltsov, M. Isobe, T. Möller, M. Hoelzel, A. Senyshyn, D. Trots, M.T. Fernández-Díaz, T. Hansen, H. Gotou, T. Yagi, Y. Ueda, V.I. Anisimov, M. Grüninger, D.I. Khomskii, M. Braden, *Physical Review Letters*, 101 (2008) 167204.
- [7] H.M. Liu, C. Zhu, C.Y. Ma, S. Dong, J.M. Liu, *Journal of Applied Physics*, 110 (2011).
- [8] J.S. Zhou, L.P. Cao, J.A. Alonso, J. Sanchez-Benitez, M.T. Fernandez-Diaz, X. Li, J.G. Cheng, L.G. Marshall, C.Q. Jin, J.B. Goodenough, *Physical Review B*, 94 (2016) 155137.
- [9] C. Adamo, V. Barone, *The Journal of Chemical Physics*, 110 (1999) 6158-6170.

- [10] Tripkovic, Vladimir, Hansen, Heine, A., Garcia-Lastra, Juan, M., Vegge, Tejs, *Journal of Physical Chemistry C Nanomaterials & Interfaces*, (2018).
- [11] V.R.S. R. Dovesi, C. Roetti, R. Orlando, C. M. Zicovich-Wilson, F. Pascale, B. Civalleri, K. Doll, N. M. Harrison, I. J. Bush, P. D'Arco, and M. Llunell, *CRYSTAL09 User's Manual* (University of Torino, Torino, 2009).
- [12] E. Castillo-Martínez, A. Durán, M.Á. Alario-Franco, *Journal of Solid State Chemistry*, 181 (2008) 895-904.
- [13] L. Valenzano, F.J. Torres, K. Doll, F. Pascale, C.M. Zicovich-Wilson, R. Dovesi, *Zeitschrift für Physikalische Chemie*, 220 (2006) 893-912.
- [14] M. Catti, G. Valerio, R. Dovesi, G. Sandrone, *Journal of Physics & Chemistry of Solids*, 57 (1996) 1735-1741.
- [15] M.D. Towler, N.L. Allan, N.M. Harrison, V.R. Saunders, W.C. Mackrodt, E. Apr, *Phys Rev B Condens Matter*, 50 (1994) 5041-5054.
- [16] H.J. Monkhorst, J.D. Pack, *Physical Review B*, 13 (1976) 5188-5192.
- [17] W.Z. Heisenberg, *Ztschrift Für Physik*, 49 (1928) 619-636.
- [18] F. Illas, I. Moreira, P.R. Rio, C. de Graaf, V. Barone, *Theoretical Chemistry Accounts: Theory, Computation, and Modeling (Theoretica Chimica Acta)*, 104 (2000) 265-272.
- [19] J. Muscat, A. Wander, N.M. Harrison, *Chemical Physics Letters*, 342 (2001) 397-401.
- [20] M.S. Hybertsen, S.G. Louie, *Physical Review B*, 34 (1986) 5390-5413.

[21] A. Georges and G. Kotliar, Rev. Mod. Phys. 68, 13 (2004).